The EMBO Journal Vol. 22 No. 19 pp. 5283–5292, 2003

Dysfunctional MreB inhibits chromosome segregation in *Escherichia coli*

Thomas Kruse, Jakob Møller-Jensen, Anders Løbner-Olesen[1] and Kenn Gerdes[2]

Department of Biochemistry and Molecular Biology, University of Southern Denmark, Odense, DK-5230 Odense M and [1]Department of Life Sciences and Chemistry, Roskilde University, DK-4000 Roskilde, Denmark

[2]Corresponding author
e-mail: kgerdes@bmb.sdu.dk

The mechanism of prokaryotic chromosome segregation is not known. MreB, an actin homolog, is a shape-determining factor in rod-shaped prokaryotic cells. Using immunofluorescence microscopy we found that MreB of *Escherichia coli* formed helical filaments located beneath the cell surface. Flow cytometric and cytological analyses indicated that MreB-depleted cells segregated their chromosomes in pairs, consistent with chromosome cohesion. Overexpression of wild-type MreB inhibited cell division but did not perturb chromosome segregation. Overexpression of mutant forms of MreB inhibited cell division, caused abnormal MreB filament morphology and induced severe localization defects of the nucleoid and of the *oriC* and *terC* chromosomal regions. The chromosomal terminus regions appeared cohered in both MreB-depleted cells and in cells overexpressing mutant forms of MreB. Our observations indicate that MreB filaments participate in directional chromosome movement and segregation.

Keywords: actin/chromosome segregation/MreB/*oriC*/*terC*

Introduction

In eukaryotic cells, the mitotic spindle apparatus segregates sister chromatids to daughter cells; however, it is largely unknown how prokaryotic cells segregate their chromosomes. Early on, the replicon model suggested that newly replicated sister chromosomes are attached to centrally located sites on the cell membrane that move towards opposite cell poles in parallel with cell elongation (Jacob *et al*., 1963). In this model, the process of chromosome segregation is essentially passive. In support of the replicon model, it was observed that nucleoids segregated slowly concomitantly with cell elongation (Van Helvoort and Woldringh, 1994; Woldringh *et al*., 1994). Based on these reports it was suggested that the coupling between transcription and translation of genes specifying co-translationally secreted proteins transiently anchors DNA to the membrane, which, in turn, slowly pulls the chromosomes apart as the cell elongates (Norris, 1995; Woldringh, 2002). In contrast, it has also been suggested that spooling of DNA through a replication factory located at mid-cell might be an important driving force in chromosome segregation (Gordon and Wright, 1998, 2000; Lemon and Grossman, 2000, 2001). RNA polymerase has also been proposed as a driving force for chromosome segregation (Dworkin and Losick, 2002). Recent experiments employing fluorescence microscopic techniques demonstrated that replicated copies of the *oriC* region moved rapidly apart from mid-cell to predetermined sites closer to the cell poles, and that this movement was independent of cell growth (Glaser *et al*., 1997; Gordon *et al*., 1997; Lewis and Errington, 1997; Webb *et al*., 1997, 1998; Niki and Hiraga, 1998; Teleman *et al*., 1998; Jensen and Shapiro, 1999; Niki *et al*., 2000). These observations are consistent with the existence of a bacterial mitotic-like apparatus, which provides the force and directionality required for the accurate segregation of chromosomal origin DNA (Sharpe and Errington, 1999; Draper and Gober, 2002). Thus, three different contemporary models have attempted to explain chromosome segregation in prokaryotic cells.

Several protein candidates have been suggested to accomplish chromosome segregation. For example, *Escherichia coli* MukB mutants exhibited a severe chromosome segregation defect (Niki *et al*., 1991), but later reports showed the MukB protein to be involved in supercoiling-dependent chromosome condensation (Weitao *et al*., 1999; Sawitzke and Austin, 2000). Most bacterial chromosomes encode homologs of plasmid-borne partitioning loci (Gerdes *et al*., 2000; Hayes, 2000; Yamaichi and Niki, 2000). For example, *soj* and *spo0J* of *Bacillus subtilis* are homologs of the P1 *parAB* genes. Soj, an oscillating protein, and Spo0J, a DNA binding protein, have many of the characteristics that might be expected for components of a chromosome segregation machinery. However, Spo0J was not needed for rapid *oriC* movement and may instead be involved in condensation and/or organization of the *oriC* proximal region (Lin and Grossman, 1998; Webb *et al*., 1998; Wu and Errington, 2002). Some γ-proteobacteria, such as *E.coli* and *Haemophilus influenzae*, do not carry *parAB* homologous loci on their chromosomes (Gerdes *et al*., 2000), yet these bacteria exhibit proper chromosome segregation. Thus, despite considerable effort, a single cellular machinery responsible for rapid movement of bacterial chromosomes has not yet been identified.

Plasmid-encoded partitioning loci (*par*) are of two types, those that encode an ATPase homologous to the oscillating Soj protein of *B.subtilis* and those that encode an actin-like ATPase (Gerdes *et al*., 2000). Recently, we obtained evidence that the DNA segregation machinery encoded by *E.coli* plasmid R1 specifies a simple prokaryotic analog of the eukaryotic spindle apparatus. The plasmid-encoded ParM protein, an actin homolog, formed F-actin-like filaments that were responsible for the

active movement of plasmid copies to opposite cell poles (Jensen and Gerdes, 1999; Moller-Jensen *et al*., 2002; van den Ent *et al*., 2002). Interestingly, ParM belongs to the actin superfamily of ATPases encompassing also the prokaryotic, filament-forming MreB protein (Bork *et al*., 1992; Jones *et al*., 2001; van den Ent *et al*., 2001). Database analyses using MreB as a query sequence revealed plasmid-encoded partitioning proteins, in both Gram-negative and Gram-positive bacteria, that are more related to the MreB family of proteins than to each other (Moller-Jensen *et al*., 2002). The plasmid-borne *mreB* homologs are encoded by *par* loci, indicating that they, as in the case of *parM* of R1, may encode filament-forming proteins that segregate plasmid DNA (Moller-Jensen *et al*., 2002).

MreB is present in all rod-shaped bacteria and is required to maintain the non-spherical shape of the cells. Thus, the disruption of *mreB* in *E.coli* and *B.subtilis* was associated with a change in cell morphology from the normal rod shape to a rounded, inflated form (Wachi *et al*., 1987; Doi *et al*., 1988; Jones *et al*., 2001). *mreB* is the first gene in the *mreBCD* operon in both *E.coli* and *B.subtilis* (Figure 1A). MreB of *B. subtilis* formed helical filamentous structures lying beneath the cell surface (Jones *et al*., 2001). Furthermore, MreB from *Thermotoga maritima* adopted the canonical actin fold and formed filaments *in vitro* (van den Ent *et al*., 2001).

Here, we investigated the role of MreB in cell-shape determination and chromosome segregation in *E.coli*. We found that MreB formed helical filaments that extended along the long axis of the cells. Flow-cytometric analyses of cells lacking MreB indicated that, in spherical cells, chromosomes segregated in pairs. Direct cytological localization of *oriC* and *terC* in round cells was consistent with paired segregation of chromosomes. Overexpression of wild-type MreB inhibited cell division but did not perturb nucleoid morphology or DNA segregation. In contrast, overexpression of mutant forms of MreB in wild-type cells inhibited cell division and concomitantly caused aberrant MreB filament morphology, impaired nucleoid segregation and severe mislocalization of the chromosomal origin and terminus regions. Thus, our results raise the possibility that MreB is directly or indirectly involved in chromosome movement and segregation.

Results

MreB forms helical structures

Polyclonal antibodies were raised against purified, affinity-tagged MreB of *E.coli* and their specificity verified by immunoblotting. In extracts of wild-type cells, the anti-MreB antibodies specifically recognized a single protein of the expected size (Figure 1B, lane 1). In extracts prepared from cells carrying an in-frame deletion in *mreB* (Δ*mreB*), no protein was detected (Figure 1B, lane 2). Control immunofluorescence microscopy (IFM) performed on Δ*mreB* cells also confirmed the specificity of the antiserum (Figure 1C). In accordance with previous results (Wachi *et al*., 1987; Doi *et al*., 1988), *E.coli* cells lacking MreB were spherical (Figure 1C) and 4′,6-diamidino-2-phenylindole dihydrochloride hydrate (DAPI) staining of DNA showed that 1–2% of the spheres were anucleate (data not shown).

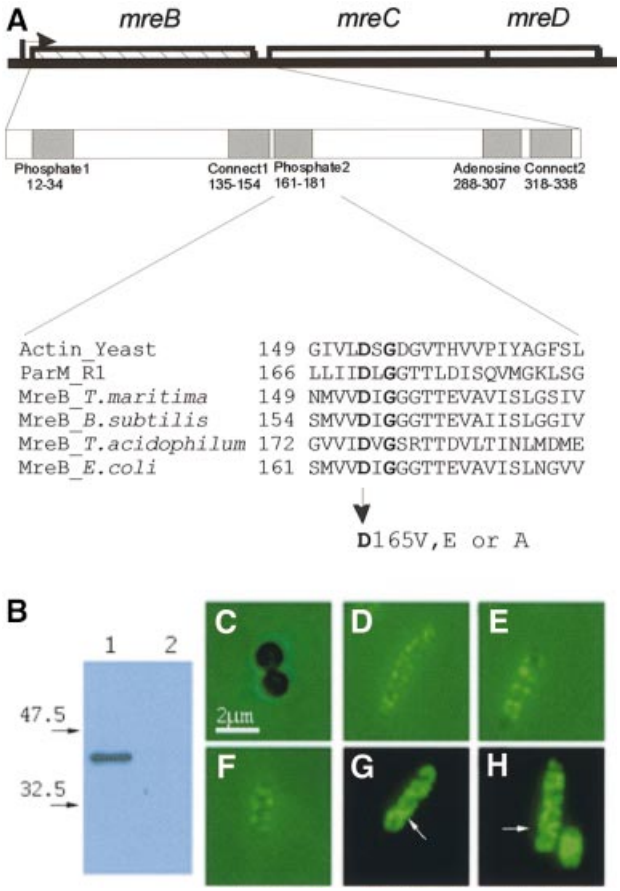

Fig. 1. Subcellular localization of the MreB protein in *E.coli*. (**A**) Schematic drawing of the *mreBCD* locus of *E.coli*. The *mreB* gene (347 codons) is shown as a hatched box, *mreC* (367 codons) and *mreD* (162 codons) as open boxes. The broken arrow pointing right-wards indicates the *mreBCD* promoter. The first enlargement shows the five regions in MreB that exhibit similarity to analogous regions present in all proteins with the actin fold (Bork *et al*., 1992). Numbers are amino acids in MreB. The second enlargement shows an alignment of the phosphate-2 regions of actin (from yeast), ParM from plasmid R1, MreBs from *T.maritima* (a deep branching eubacterium), *B.subtilis*, *Thermoplasma acidophilum* (an archaeon) and *E.coli*. Conserved amino acids are in bold. Amino acid changes at position +165 in the phosphate-2 region of MreB of *E.coli* are indicated. (**B**) Immunoblot showing the specificity of the affinity purified anti-MreB antibodies. Lane 1, protein extract from wild-type cells (MC1000); lane 2, MC1000Δ*mreB*. Molecular weight markers are shown to the left. (**C**–**H**) Subcellular localization of MreB visualized by combined phase-contrast and immunofluorescence microscopy using affinity purified anti-MreB antibodies. (C) Cells of MC1000Δ*mreB*; (D–F) cells of MC1000; (G and H) cells of MC1000 visualized by fluorescence microscopy in the absence of phase-contrast. Arrows point to helical structures. Cells were grown at 30°C in AB glycerol medium supplemented with 0.025% casamino acids.

IFM of wild-type cells using the MreB-specific antibodies revealed a range of distinct structures that included transverse bands and pairs of dots that were distributed in a criss-cross pattern extending along the long axis of the cells (Figure 1D–H). Reduction in light intensity enabled the visualization of structures that were clearly helical (Figure 1G and H). These results suggested that the MreB structures located close to the cell surface. As MreB is a cytosolic protein, the helices probably located to the inner surface of the cytoplasmic membrane. The helical pitch based on measurements of 95 clearly defined structures was estimated to be 0.46 ± 0.08 μm.

To assess whether a sufficient number of MreB molecules were present to account for the formation of these helical structures, the cellular amount of MreB was determined by quantitative immunoblotting. The amount of MreB was estimated as ~17 000 molecules/cell in slowly growing cells and ~40 000 molecules/cell in rapidly growing cells (data not shown). Assuming a longitudinal monomer spacing of 51 Å within MreB filaments (van den Ent *et al*., 2001), there seemingly is sufficient MreB to form a filament that could encircle the cell several times. We conclude that MreB monomers assemble into, or adhere to, helical filamentous structures that extend along the longitudinal axis of *E.coli* cells just beneath the surface of the cytoplasmic membrane.

In *B.subtilis*, depletion of MreB led to a rounded, inflated cell morphology and eventually to cell lysis (Jones *et al*., 2001). Thus, in *B.subtilis*, *mreB* is essential. Using a conditional *mreB* expression system, we found that depletion of MreB conferred a spherical cell morphology and a significant reduction (5-fold) in cell plating efficiency (to be published elsewhere).

MreB deficient cells contain even numbers of replication origins

Numbers of replication origins in wild-type and Δ*mreB* cells were determined by flow cytometry. The method used takes advantage of the fact that rifampicin stops new rounds of replication initiations at *oriC* but allows ongoing replication forks to finish. Wild-type cells grown in minimal medium had a doubling time of 120 min and contained predominantly one or two origins (Figure 2A). When grown in rich medium, wild-type cells had a doubling time of 24 min and contained four or eight origins. This is in agreement with previously published results (Skarstad *et al*., 1986). In contrast, Δ*mreB* cells grown in minimal medium had a doubling time of 150 min and contained two or four origins (Figure 2A). When grown in rich medium, Δ*mreB* cells had a doubling time of 39 min and contained 2, 4, 6, 8, 10, 12 or even 14 origins. The predominant classes of cells had 4, 6, 8 or 10 origins. These observations are consistent with the proposal that, in Δ*mreB* cells, the origins segregated in pairs. Even more importantly, the distribution indicates that the paired chromosomes segregated randomly.

Cell size distributions obtained by flow cytometry showed that the average size of Δ*mreB* cells was approximately two times that of wild-type cells in rich and poor medium. Thus, both cell size and DNA content were elevated in Δ*mreB* cells. Mini-cell producing strains (*minB*) also had an ~2-fold increased cell size (de Boer *et al*., 1989; this work). We investigated the *oriC* distribution pattern in PB103 (wild type) and PB114 (*minB*) by flow cytometry (Figure 2B). Slowly growing *minB* cells had two or four origins, whereas rapidly growing *minB* cells had 4, 8 or 16 origins, but never 6, 10 or 12. Thus, *minB* cells exhibited the 2^n distribution of replication origins similar to that of wild-type cells, indicating that the chromosome segregation machinery was operational even with an increased number of chromosomes. We conclude that the even number of replication origins of MreB-depleted cells is not a simple consequence of an increased number of chromosomes and cell volume.

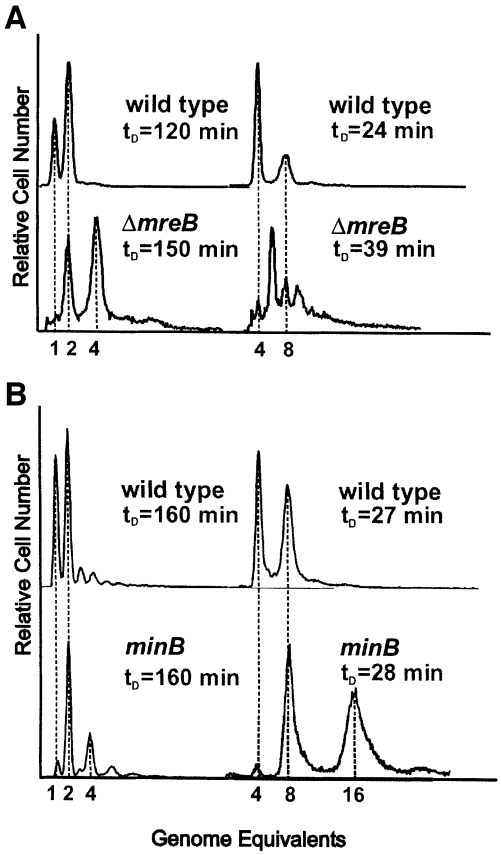

Fig. 2. Number of replication origins in single cells counted by flow cytometry. (**A**) Shown are flow cytometric histograms of *E.coli* strains MC1000 (wild type) and MC1000Δ*mreB* obtained after 4 h of treatment with rifampicin. Rifampicin was added to inhibit new replication initiations at *oriC* and to allow for run-out synthesis of ongoing rounds of DNA replication. DNA was stained with ethidium bromide. Left, cells were grown in AB glycerol minimal medium at 37°C. Right, the cells were grown in LB medium. The cell mass doubling times at the times of addition of rifampicin are indicated. (**B**) Flow-cytometric histograms of PB103 (wild type) and PB114 (*minB*) cells grown as described above.

Subcellular localization of oriC and terC in ΔmreB cells

To determine the subcellular localization of specific chromosomal regions, the bacteriophage P1 partitioning site, *parS*, was inserted near *oriC* (in the *bglF* gene at 84 min) or *terC* (in the *relBE* operon at 34 min) in both wild-type and Δ*mreB* cells (see Materials and methods). The ParB protein of plasmid P1 binds to the *parS* site and spreads outward to cover adjacent sequences (Rodionov *et al*., 1999). When a Gfp–ParB fusion protein was expressed from a co-resident plasmid, the DNA region harboring *parS* formed a bright fluorescent signal, which thus allowed visualization of *parS* containing DNA segments (Li *et al*., 2002). Gfp–ParB synthesis was induced for 3 h of growth before inspection by fluorescence microscopy.

In minimal medium, wild-type cells had either one *oriC* focus at mid-cell or two foci near the one-quarter and three-quarter positions (Figure 3Aa and b). In rich medium, newborn wild-type cells had two *oriC* foci located at the one-quarter and three-quarter positions, whereas predivisional cells had four foci evenly distributed

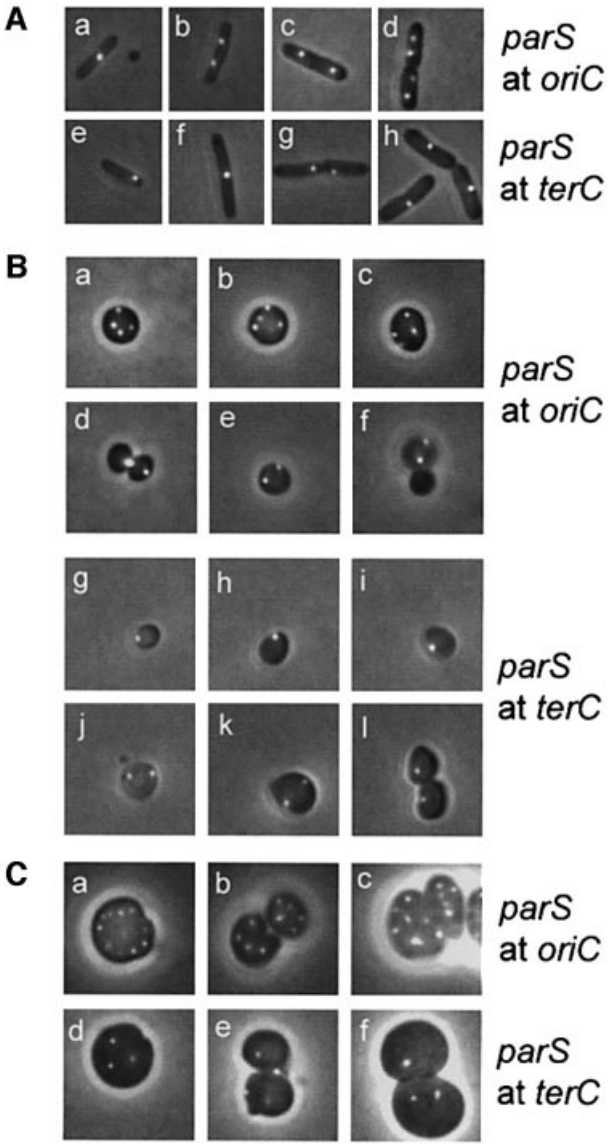

Fig. 3. Subcellular localization of *oriC* and *terC*. *oriC* and *terC* regions were visualized by Gfp–ParB nucleation on *parS* sites inserted in *bglF* (near *oriC*) or in *relBE* (near *terC*). All strains shown contained plasmid pTK536 that expressed a Gfp–ParB fusion protein. Cells were grown at 37°C in AB glycerol or LB medium with a doubling time of 145 or 27 min (wild type) and 174 or 44 min (Δ*mreB*), respectively. (**A**) Expression of Gfp–ParB was induced with 0.2% arabinose 180 min before inspection. (a and b) MC1000 with *parS* inserted near *oriC* grown in AB glycerol. (c and d) Same strain grown in LB medium. (e–g) MC1000 with *parS* inserted near *terC* grown in AB glycerol. (h) Same strain grown in LB medium. (**B**) MC1000Δ*mreB* cells with *parS* near *oriC* (a–f) or *terC* (g–l) grown in AB glycerol. (**C**) MC1000Δ*mreB* cells with *parS* inserted at *oriC* (a–c) or *terC* (d–f) grown in LB medium.

(Figure 3Ac and d). Newborn cells invariably had one *terC* focus, in both minimal and rich media, indicating that terminus segregation and septum formation occur in parallel. In minimal medium, the focus was located near a cell pole (Figure 3Ae), whereas in rich medium, the *terC* focus was always located at mid-cell (Figure 3Ah). Predivisional cells grown in minimal medium either had one centrally located *terC* focus (Figure 3Af) or two foci located close to each other at mid-cell (Figure 3Ag). These patterns of *oriC* and *terC* localization in wild-type cells are consistent with previous observations (Niki *et al*., 2000; Li *et al*., 2002), thus validating the Gfp–ParB/*parS*-based method of DNA detection used here.

Grown in minimal medium, Δ*mreB* cells invariably had two (68%) or four (31%) *oriC* foci (Figure 3Ba–f), consistent with the number of replication origins counted by flow cytometry (Figure 2A) and with the inference that the chromosomes segregated in pairs. Predivisional cells usually exhibited a non-symmetrical, random *oriC* localization pattern (Figure 3Ba–c) or even clustering at the site of division (Figure 3Bd). New-born cells with two *oriC* foci were also seen (Figure 3Be and f). The presence of spheres without an *oriC* focus indicated loss of the entire chromosome during cell division (Figure 3Bf). Spherical cells grown in rich medium had many, highly irregularly spaced *oriC* foci in a pattern too complex to be quantified (Figure 3Ca–c). Many cells had more than 14 origins. These cells were not detected by flow cytometry (Figure 2A), probably due to their disintegration during processing of the cell samples.

Interestingly, slowly growing Δ*mreB* cells only had one (71%) or two *terC* foci (28%) (Figure 3Bg–l). Despite thorough examination, such cells never had more than two *terC* foci. In these cells, growing with a 174 min doubling time, we determined the replication time for the chromosome (C-period) to be 70 ± 5 min. Thus, cells had ample time to finish chromosome replication within one doubling time and therefore contained four copies of *oriC* as well as *terC* at the time of cell division. It is therefore conceivable that each *terC* focus in predivisional cells represents two *terC* regions in close proximity. Fast growing Δ*mreB* cells had an irregular *terC* focus pattern, too complex to be quantified (Figure 3Cd–f). However, these cells clearly had fewer *terC* than *oriC* foci, also consistent with cohesion of the terminus regions.

Mutant MreB proteins perturb wild-type MreB filament morphology

Next, we investigated MreB filament morphology in wild-type cells expressing wild-type or mutant MreBs ectopically. The conserved aspartic acid residue at position 165 in MreB is located in the phosphate-2 domain that forms part of the ATP binding domain in all members of the actin ATPase family (Bork *et al*., 1992; see Figure 1A). Mutations at the similar position in ParM of plasmid R1 inactivates the *par* locus and the mutant ParM protein exhibits *trans*-dominance (Jensen and Gerdes, 1997). Using site-directed mutagenesis, the aspartic acid residue was changed to valine (a change to an uncharged amino acid of similar size), to glutamate (a conservative change) and to alanine (a change to a small uncharged amino acid). The mutated and native *mreB* genes were cloned downstream of the isopropyl-β-D-thiogalactopyranoside (IPTG)-inducible pA1/O3/O4-promoter in the low-copy-number expression vector pNDM220 (Gotfredsen and Gerdes, 1998). To verify that the mutant forms of MreB were actually defective, we tested whether the proteins were able to complement the cell-shape defect conferred by the Δ*mreB* deletion. Although a wide range of IPTG concentrations were used for induction, even the wild-type *mreB* allele did not fully complement the Δ*mreB* mutation (data not shown). The reason for this lack of complement-

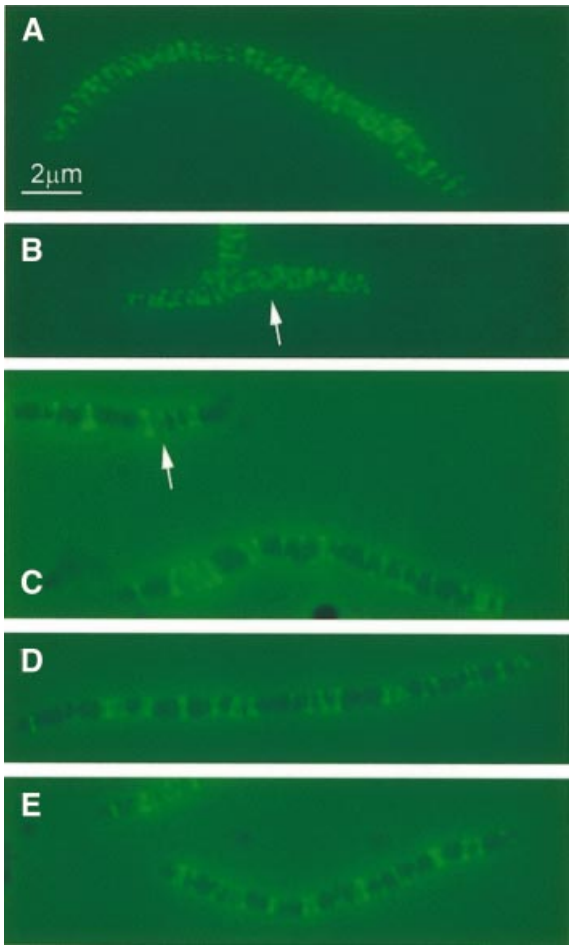

Fig. 4. MreB localization in elongated cells visualized by immunofluorescence microscopy. Subcellular localization of MreB in wild-type cells treated with cephalexin or in wild-type cells expressing native or mutated forms of *mreB* present in the low-copy-number expression vector pNDM220. Cells were grown at 30°C in AB glycerol medium supplemented with 0.025% casamino acids. Cells were induced with 100 μM of IPTG for five mass doublings. Localization of MreB was performed using affinity purified anti-MreB antibodies and combined phase-contrast and immunofluorescence microscopy. Arrows point to unmistakable helical structures. (**A**) Cells of MC1000 (*mreBCD*$^+$) were treated with 10 μg/ml cephalexin for three mass doublings prior to microscopy. (**B**) MC1000/pTK505 (wild-type *mreB*); (**C**) MC1000/pTK509 (*mreB165V*); (**D**) MC1000/pTK510 (*mreB165E*); (**E**) MC1000/pTK511 (*mreB165A*).

ation is not known, but a similar lack of complementation was seen in the case of *B.subtilis mreB* (Jones *et al*., 2001). To circumvent this problem, we cloned the entire *mreBCD* operon into our expression vector. In this case, transcription of the wild-type *mreBCD* operon fully complemented the defects of the Δ*mreB* mutation (data not shown). Transcription of the *mreBCD* operon encoding the mutant forms of MreB described above, however, did not complement the Δ*mreB* deletion (data not shown). Thus, the single amino acid changes at +165 in all cases inactivated MreB.

Wild-type cells carrying wild-type or mutant forms of *mreB* under the control of the IPTG-inducible promoter were grown at an intermediate level of induction (100 μM IPTG) for five mass doublings. For convenience, the strains were denoted: wild type/*mreB165D*, wild type/*mreB165V*, wild type/*mreB165E* and wild type/*mreB165A*, respectively. Combined phase-contrast and IFM were performed on the merodiploid cells using MreB-specific antibodies. Overexpression of the wild-type form of MreB resulted in the formation of elongated cells, indicating that cell division was inhibited (Figure 4B). This effect was in agreement with previous findings (Wachi and Matsuhashi, 1989). MreB formed helical structures that were present over the entire length of the elongated cells, very similar to the MreB filaments seen in wild-type cells treated with the cell division inhibitor cephalexin (Figure 4A). Wild-type cells expressing mutant MreB proteins ectopically also resulted in the formation of elongated cells, again indicating a defect in cell division (Figure 4C–E). MreB filament formation was, however, perturbed in these cells. It was still possible to detect clearly defined fluorescent structures as dots, transverse bands and even helices, but the helices were unevenly distributed, leaving parts of the cells with little or no detectable MreB signal (helical structures are indicated with arrows in Figure 4B and C). Thus, ectopic expression of mutant MreB proteins in a wild-type background interfered with MreB filament formation and cell division while the rod shape of the cells was maintained.

Interestingly, the diameter of the elongated cells expressing the mutant forms of MreB varied significantly (Figures 4–6). Thus, wild-type cells treated with cephalexin and wild-type cells expressing native MreB all had an average diameter of 0.83 ± 0.04 μm. In contrast, wild-type cells expressing MreB165E and MreB165A had significantly smaller diameters (0.69 ± 0.03 and 0.60 ± 0.06 μm, respectively), whereas cells expressing MreB165V had a significantly larger diameter (1.09 ± 0.07 μm). Thus, MreB controls not only cell length but also cell width.

Interference with MreB filament formation results in aberrant nucleoid morphology and positioning

Nucleoid morphology was visualized by DAPI staining. Slowly growing wild-type cells contained one centrally located nucleoid (Figure 5A). Treatment of these cells with cephalexin for two to three mass doublings resulted in filamentous cells with nucleoids that were well defined and evenly spaced (Figure 5B). A similar cell and nucleoid morphology was observed in cells overexpressing wild-type MreB, indicating that chromosome segregation occurred despite the inhibition of cell division (Figure 5C). MreB proteins with the aspartic acid residue at +165 substituted with valine, glutamate or alanine expressed in a wild-type background produced elongated cells as described above. In these cells, however, nucleoid morphology was highly perturbed (Figure 5D–F). In all three cases, the nucleoids appeared as single diffuse and elongated entities without any clearly demarcated borders. We conclude that interference with MreB filament formation prevented nucleoid separation.

The MreB filament defect causes abnormal localization of oriC and terC

Using the Gfp–ParB/*parS* system described above, we investigated the localization patterns of *oriC* and *terC* in cells overexpressing either wild-type or mutant forms of MreB in an otherwise wild-type background. MreB and

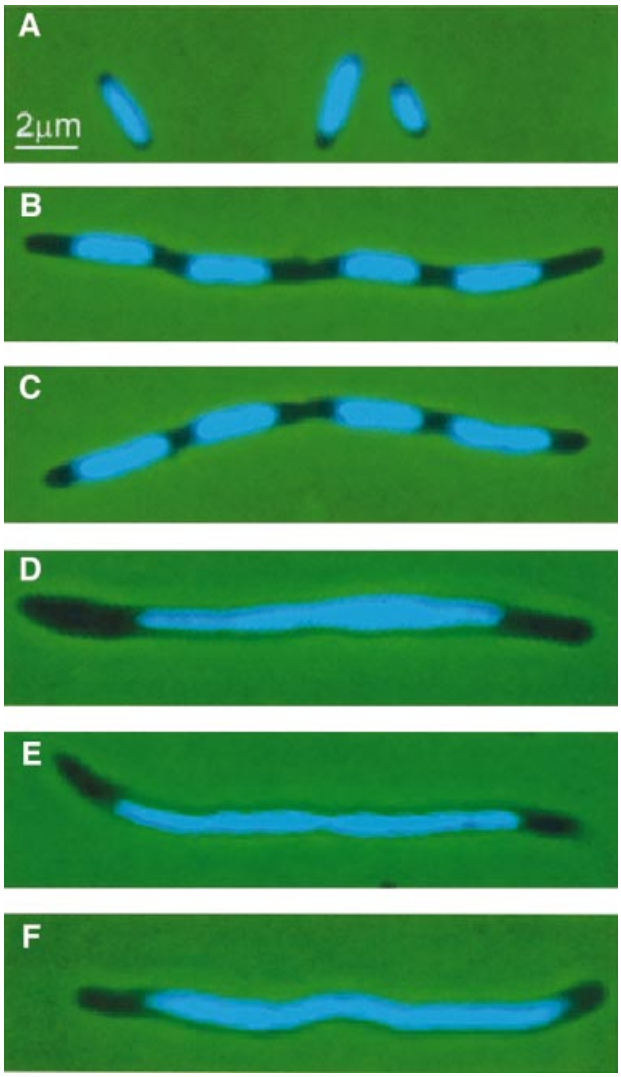

Fig. 5. Inhibition of nucleoid segregation by mutant forms of MreB. Nucleoid distribution in cells of MC1000 (*mreBCD*$^+$) treated with cephalexin or MC1000 expressing native or mutated forms of *mreB* present in the expression vector pNDM220. Cells were grown at 30°C in AB glycerol medium supplemented with 0.025% casamino acids and stained with DAPI. MreB synthesis was induced with IPTG (100 μM) for five mass doublings. (**A**) MC1000 wild-type cells grown exponentially; (**B**) MC1000 wild-type cells were treated with 10 μg/ml cephalexin for three mass doublings prior to microscopy; (**C**) cells of MC1000/pTK505 (wild-type *mreB*); (**D**) MC1000/pTK509 (*mreB165V*); (**E**) MC1000/pTK510 (*mreB165E*); (**F**) MC1000/pTK511 (*mreB165A*).

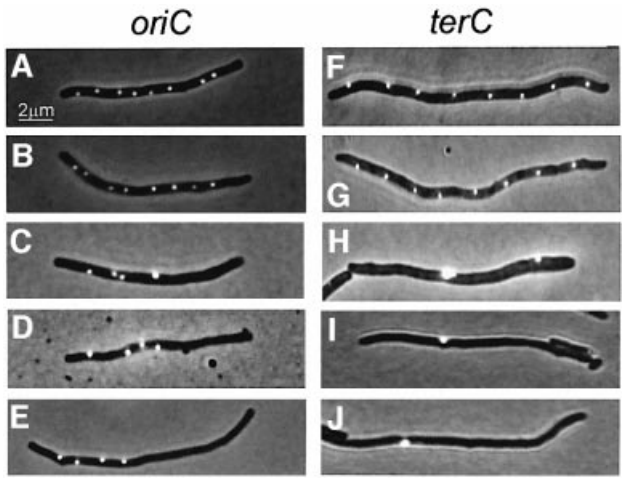

Fig. 6. Defect localization of *oriC* and *terC* in cells expressing mutant forms of MreB. Localization of *oriC* and *terC* by Gfp–ParB labeling in wild-type cells treated with cephalexin or in wild-type cells expressing native or mutated forms of *mreB* present in expression vector pNDM220. Cells were grown at 30°C in AB glycerol medium supplemented with 0.025% casamino acids. MreB synthesis was induced with IPTG (100 μM) for five mass doublings and Gfp–ParB synthesis (from pTK536) with 0.2% arabinose for 180 min. (A–E) Cells with *parS* inserted into *bglF* (near *oriC*); (F–J) cells with *parS* inserted into *relBE* (near *terC*). (**A**) MC1000*bglF*::*parS*/pTK536 cells treated with 10 μg/ml cephalexin for three mass doublings; (**B**) MC1000*bglF*::*parS*/pTK536/pTK505 (wild-type *mreB*); (**C**) MC1000*bglF*::*parS*/pTK536/pTK509 (*mreB165V*); (**D**) MC1000*bglF*::*parS*/pTK536/pTK510 (*mreB165E*); (**E**) MC1000*bglF*::*parS*/pTK536/pTK511 (*mreB165A*); (**F**) MC1000*relBE*::*parS*/pTK536 treated with 10 μg/ml cephalexin; (**G**) MC1000*relBE*::*parS*/pTK536/pTK505 (wild-type *mreB*); (**H**) MC1000*relBE*::*parS*/pTK536/pTK509 (*mreB165V*); (**I**) MC1000*relBE*::*parS*/pTK536/pTK510 (*mreB165E*); (**J**) MC1000*relBE*::*parS*/pTK536/pTK511 (*mreB165A*).

Gfp–ParB syntheses were induced as described above for Figures 3 and 4, respectively. In cells overexpressing wild-type MreB, the origin- and terminus-proximal *parS* sites were observed to distribute as multiple, equally spaced foci along the long axis of the elongated cells (Figure 6B and G). A similar origin and terminus distribution was observed in cells treated with cephalexin (Figure 6A and F). These observations indicate that, in elongated cells, cell division was dispensable for the segregation and regular distribution of *oriC* and *terC* proximal regions.

In contrast, in the wild type/*mreB165V*, wild type/*mreB165E* and wild type/*mreB165A* strains, the origin-proximal *parS* sites were found to be severely dislocated (Figure 6C–E). Furthermore, the *oriC* proximal foci emitted a brighter fluorescent signal in these cells as compared with cells overexpressing wild-type MreB or cells treated with cephalexin, suggesting that at least some of the foci represented more than a single origin region. This result indicates a defect in the segregation of newly replicated copies of the *oriC* region.

The localization defect of the terminus region was even more dramatic (Figure 6H–J). Here, ectopic expression of the mutant MreBs caused the terminus regions to appear as single large and brightly fluorescent aggregates in the majority of the cells. Thus, interference with MreB function caused terminus cohesion.

Discussion

We show here that native MreB forms helical filaments that are required to maintain the non-spherical form of *E.coli* cells. Recently, a YFP–MreB fusion protein was shown to form helices similar to the ones described here (Shih *et al*., 2003). In *B subtilis*, MreB formed large, right-handed helices that were required to maintain cell shape (Jones *et al*., 2001). Mbl, a helix-forming MreB paralog in *B.subtilis*, was also required to maintain the shape of the cells (Jones *et al*., 2001; Carballido-Lopez and Errington, 2003) and was responsible for directing lateral cell wall synthesis in a helical pattern (Daniel and Errington, 2003). The MreB and Mbl filaments were responsible for width and linear axis control, respectively. We found here that expression of mutant forms of *E.coli* MreB resulted in

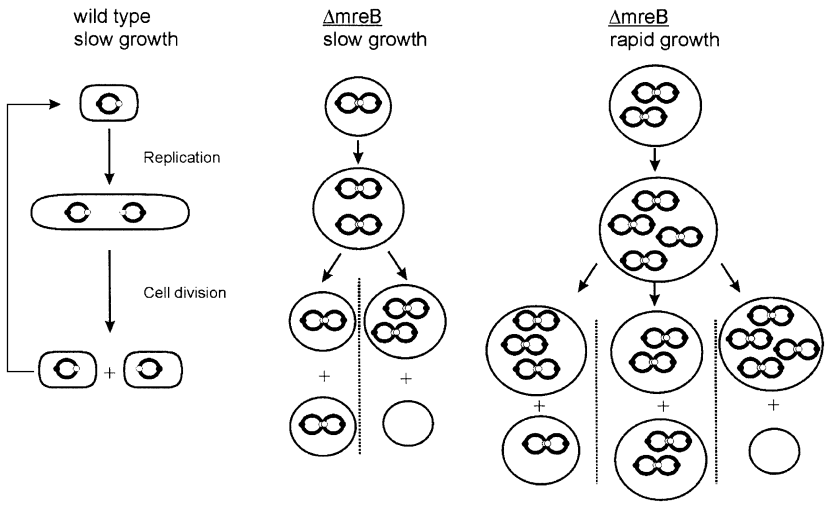

Fig. 7. Pairing explains the chromosome segregation pattern in cells lacking MreB. Chromosomes stay paired in Δ*mreB* cells (cohesion). The model assumes that replication allows separation of the old chromosomes and that the newly replicated sister chromosomes stay together as pairs. Pairing explains the even number of chromosomes in the Δ*mreB* strain seen at all growth rates. During division of Δ*mreB* cells, paired chromosomes segregate randomly, thus leading to anucleate cells and to cells with an even number of chromosomes. The lack of coordination of chromosome segregation also explains the broad copy-number distribution of chromosomes seen in the Δ*mreB* cells. The schematic does not show all possible combinations of the number of chromosomes in rapidly growing Δ*mreB* cells. Symbols: chromosomes are shown as large circles, origins of replication as closed dots and termini as open dots. For simplicity, chromosomes are shown as full circles and the figure does not take ongoing replication into account.

altered width of the cells (Figures 4–6). Thus, MreB of *E.coli* also appears to control cell width. *E.coli* does not have MreB paralogs, suggesting that MreB of *E.coli* simultaneously controls cell width and linear axis. We conclude that the MreB family of proteins forms helical filaments pivotal in maintaining cell morphology in both Gram-negative and -positive bacteria.

It is not known how MreB filaments determine cell shape. The morphology of *E.coli* Δ*mreB* cells is very similar to that of cells lacking either penicillin-binding-protein-2 (PBP2) or RodA. In both cases, lateral cell wall synthesis was impaired (De Pedro *et al*., 2001). One attractive model is that MreB provides a scaffold that organizes the peptidoglycan synthesizing machinery (including PBP2) during cell elongation and thereby coordinates lateral cell wall growth with extension of the cell interior (Carballido-Lopez and Errington, 2003; Daniel and Errington, 2003).

MreB functions in chromosome segregation

The homology between MreB and the DNA segregation protein ParM of plasmid R1 inspired us to investigate whether MreB plays a role in chromosome segregation. The number of replication origins (*oriC*) in individual cells was measured by two independent methods, flow cytometry and fluorescence microscopy. Both methods showed that, in Δ*mreB* cells, the origin distribution was consistent with the proposal that origins segregated in pairs. Moreover, the *oriC* localization pattern was highly disordered in Δ*mreB* cells, especially at rapid growth conditions during which *terC* localization was disordered as well. A mini-cell producing strain, which also had an increased cell volume and number of chromosomes per cell, exhibited a normal *oriC* distribution pattern (Figure 2B). Thus, the disordered *oriC* distribution pattern in MreB-depleted cells was not a mere consequence of an increased chromosome number per cell.

In contrast, slowly growing Δ*mreB* cells had a *terC* focus number very similar to that of wild-type cells: small cells had one *terC* focus, while large, pre-divisional cells had two *terC* foci (Figure 3). Thus, in single cells, the number of *oriC* foci was increased without a concomitant increase in the number of *terC* foci. An increased chromosomal replication time of Δ*mreB* cells could explain the increased *oriC*/*terC* focus-ratio in these cells. Therefore, we measured the replication time in wild-type and Δ*mreB* cells by flow cytometry. However, the replication time of the chromosome was not significantly altered in Δ*mreB* cells (determined to be 70 ± 5 min for both strains; data not shown). Hence, we favor the alternative explanation that the increased *oriC*/*terC* focus ratio in Δ*mreB* cells reflects cohesion of the chromosomal termini regions. The cause of terminus cohesion is not known. However, terminus cohesion may be a consequence of a dysfunctional chromosome segregation machinery.

Overexpression of wild-type MreB inhibited cell division (Figures 4B and 5C). The MreB helix pattern in these elongated cells was indistinguishable from that seen in elongated cells obtained by cephalexin treatment (Figure 4A versus B). Even more importantly, the nucleoids were evenly distributed along the long axis of the elongated cells in both cases (Figure 5B and C). In stark contrast to this 'wild-type' nucleoid distribution pattern, overexpression of mutant MreB prevented nucleoid separation (Figure 5D–F) and at the same time perturbed the MreB filament pattern (Figure 4C–E). In cells expressing mutant MreB, bulk DNA was located in one large, coalesced nucleoid in the middle of the elongated cells. Concomitantly, *oriC* localization was highly disordered and the *terC* regions did not separate at all in these cells (Figure 6), indicating terminus cohesion. Thus, mutations in the phosphate-2 regions of the actin homologs ParM and MreB conferred DNA segregation

Table I. Plasmids used and constructed

Plasmid	Genotypes/plasmid properties[a]	Source or reference
pBAD33	p15A *cat araC* pBAD	Guzman *et al.* (1995)
pEGFP	pUC p*lac*::*egfp bla*	Clontech
pKD3	*cat*, template plasmid	Datsenko and Wanner (2000)
pKD46	*bla*, λ Red recombinase expression	Datsenko and Wanner (2000)
pNDM220	mini-R1 *bla lacI*^{q} pA1/O4/O3	Gotfredsen and Gerdes (1998)
pMG25	pUC *bla lacI*^{q} pA1/O4/O3	Laboratory collection
pTK500	pMG25 pA1/O4/O3::*his8*::*mreB bla*	This work
pTK505	pNDM220 pA1/O4/O3::*mreB bla*	This work
pTK509	pTK505 pA1/O4/O3::*mreB165V bla*	This work
pTK510	pTK505 pA1/O4/O3::*mreB165E bla*	This work
pTK511	pTK505 pA1/O4/O3::*mreB165A bla*	This work
pTK512	pMG25 pA1/O4/O3::*mreBCD bla*	This work
pTK514	pTK512 pA1/O4/O3::*mreB165VmreCD bla*	This work
pTK515	pTK512 pA1/O4/O3::*mreB165EmreCD bla*	This work
pTK516	pTK512 pA1/O4/O3::*mreB165AmreCD bla*	This work
pTK521	pNDM220 pA1/O4/O3::*mreBCD bla*	This work
pTK523	pTK521 pA1/O4/O3::*mreB165VmreCD bla*	This work
pTK524	pTK521 pA1/O4/O3::*mreB165EmreCD bla*	This work
pTK525	pTK521 pA1/O4/O3::*mreB165AmreCD bla*	This work
pTK526	pEGFP p*lac*::*gfp*::*parB bla*	This work
pTK536	pEGFP p*lac*::SD-*parM*::*gfp*::*parB bla*	This work
pTK536	pBAD33 pBAD::SD-*parM*::*gfp*::*parB cat*	This work

[a]*cat* denotes the chloramphenicol transacetylase gene; *bla* the β-lactamase gene.

defects in both cases—a striking coincidence. Taken together, our observations raise the possibility that MreB filaments participate directly or indirectly in chromosome segregation. However, we do not exclude the possibility that terminus cohesion reflects interference with the function of FtsK, a protein that couples separation of termini with completion of the divisional septum (Aussel *et al*., 2002).

A model that explains all our observations regarding chromosome segregation in MreB depleted cells is shown in Figure 7. The model proposes that lack of MreB leads to sister chromosome cohesion, most likely via cohesion of the chromosome terminus regions. Newly replicated chromosomes stay together until a new round of replication leads to resolution of the pairs. However, the newly replicated chromosomes stay paired and the chromosomes will therefore, in all cases, segregate as paired structures. We find that our results strongly indicate that the paired chromosomes segregate randomly as depicted in Figure 7. This is because random segregation of paired chromosomes would lead to (spherical) cells containing two, four, six, etc., chromosomes. Thus, the model simultaneously explains the flow-cytometric data (Figure 2A), and the *oriC* and *terC* localization patterns (Figure 3B).

How do mutant MreB proteins interfere with MreB filament formation and function? MreB from *T.maritima* formed filaments *in vitro* (van den Ent *et al*., 2001), and it is reasonable to assume that the filamentous structures observed here (Figure 4) and by Jones *et al*. (2001) consist of MreB. We infer that the functionally inactive mutant MreB proteins retained the ability to interact with wild-type MreB and, doing so, interfered with its proper function. This interpretation is supported by the altered MreB filament morphology seen when mutant MreB proteins were expressed in wild-type cells (Figure 4C–E). In the case of the filament-forming ParM protein of plasmid R1, point mutations at the same position in the phosphate-2 region simultaneously inactivated its ATPase activity and its ability to sustain plasmid DNA segregation (Jensen and Gerdes, 1997; Moller-Jensen *et al*., 2002). Strikingly, the mutant ParM proteins also interfered with the function of wild-type ParM, indicating that wild-type and mutant ParM formed inactive complexes (Jensen and Gerdes, 1997).

What is the role of MreB in chromosome segregation? It is possible that the defect shape of Δ*mreB* cells affects chromosome segregation indirectly. However, the observation that rod-shaped cells expressing mutant MreBs do not segregate their chromosomes properly indicates that it is not the shape of the spherical cells *per se* that causes the chromosome segregation defect. Our results raise the possibility that MreB plays a more direct role in chromosome segregation analogous to what has been described for its plasmid-encoded homolog ParM (Moller-Jensen *et al*., 2002; van den Ent *et al*., 2002). One straightforward interpretation is that the actin-like MreB filaments actively move chromosomal DNA in opposite directions in coordination with lateral cell wall growth. Such a mechanism would require that MreB filaments are dynamic. This was shown recently to be the case for the Mbl filaments of *B.subtilis* (Carballido-Lopez and Errington, 2003).

Materials and methods

Bacterial strains

The standard *E.coli* K-12 strain MC1000 [*araD139* Δ(*ara*, *leu*)7697 Δ*lacX*74 *galU galK atrA*] was used throughout (Casadaban and Cohen, 1980). MC1000Δ*mreB* contains an in-frame deletion in which all but the 3′ and 5′ 36 base pairs were deleted. The deletion was constructed by employing the 'one-step inactivation of chromosomal genes' procedure (Datsenko and Wanner, 2000). Briefly, a PCR fragment containing the *cat* gene flanked by two FLP recognition targets (FRT) was generated using the oligonucleotides KO-1 and KO-2 with pKD3 as template (sequences of DNA oligonucleotides are available upon request). This PCR product contains 36 nucleotide extensions that are homologous to the 3′ and 5′ 36

base pairs of *mreB*. The PCR fragment were introduced into BW25113/pKD46, resulting in insertion of the FRT *cat* FRT cassette in the *mreB* gene. The *mreB* disruption was transduced into MC1000 and the resistance gene deleted. The structure of the recombinants was confirmed by PCR analysis. The mini-cell producing strain PB114 (*minB*::*aphA*) was donated by Piet de Boer (de Boer *et al*., 1989).

Insertion of parS at oriC and terC

Using pKD3 (Datsenko and Wanner, 2000) as a template, the *cat* gene flanked by two FRT sites was PCR amplified using primers O1 and O2. The PCR fragment was cut with *Eco*RI and *Bam*HI and inserted into pMG25 resulting in pTK532. Using P1 as a template, the *parS* sequence was PCR amplified using primers O3 and O4. This PCR fragment was digested with *Bam*HI and *Hin*dIII and inserted into pTK532 resulting in pTK533. Plasmid pTK533 contains *parS* inserted downstream of the *cat* gene flanked by two FRT sites. OriC-1 and OriC-2 contain two flanking 36 nucleotide extensions homologous to sites in the *bglF* gene at 84 min (near *oriC*). TerC-1 and TerC-2 contains two flanking 36 nucleotide extensions homologous to sites in the *relBE* operon at 34 min (near *terC*). These sets of oligonucleotides were used to generate PCR fragments containing *parS* linked to the *cat* gene and the two FRT sites using pTK533 as a template. The PCR fragments were introduced into cells of BW25113. The *bglF*::*parS* and *relBE*::*parS* fusions were transduced to appropriate strains. The final strains were MC1000 *bglF*::*parS*, MC1000 *relBE*::*parS*, MC1000Δ*mreB bglF*::*parS* and MC1000Δ*mreB relBE*::*parS*.

Plasmids used and their construction

The plasmids used here are listed in Table I, and their construction is described in the Supplementary data, available at *The EMBO Journal* Online.

Growth conditions and media

To express ParB–Gfp, cells containing pTK536 and the relevant plasmids were grown in AB minimal medium supplemented with 0.2% glycerol and 1 μg/ml thiamine or in AB minimal medium supplemented with 0.2% glycerol, 0.025% casamino acids and 1 μg/ml thiamine, as indicated. Expression of the ParB–Gfp fusion protein was induced by 0.2% arabinose. Induction for 180 min before microscopy yielded optimal results. For IFM, cells were grown in AB minimal medium.

Expression in MC1000 of native or mutant MreB from plasmids pTK505 (expresses native MreB), pTK509 (MreB165V), pTK510 (MreB165E) and pTK511 (MreB165A) was induced by adding 100 μM of IPTG. Cephalexin was added to a final concentration of 10 μg/ml.

Quantification of MreB by western blotting

For western blots, cells were grown in AB minimal medium with 0.2% glycerol, 0.025% casamino acids and 1 μg/ml thiamine to an OD_{450} of 0.3. Relative protein concentrations were determined by standard immunoblotting.

Fluorescence microscopy

Cells expressing the ParB–Gfp fusion protein were immobilized on microscope slides using a thin film of agarose (Glaser *et al*., 1997). Cells were observed with a Leica DMRA fluorescence and phase-contrast microscope with a Leica PL APO 100×/1.40 objective. Pictures were obtained with a Leica DC500 colour CCD camera and stored digitally using the Leica IM500 computer software.

For IFM, cells were grown in AB glycerol medium. Cells containing pTK505, pTK509, pTK510 and pTK511 were grown for four to five doublings with 100 μM IPTG. Cells were fixed and stained as described previously (Harry *et al*., 1995) with the following modifications: cells were fixed in phosphate-buffered saline (PBS) (pH 7.4) with a final concentration of 4% paraformaldehyde and 0.02% glutaraldehyde and immobilized on multi-well glass slides (VWR International) coated with poly-L-lysine. Permeabilization of cells was performed with a solution of freshly prepared 5 μg/ml lysozyme in PBS for 10 min. Affinity-purified anti-MreB antibodies and secondary Alexa488-conjugated goat anti-rabbit IgG antibodies (Molecular Probes) were used at 1:100 and 1:200 dilutions, respectively.

Flow cytometry

For the determination of numbers of origins per cell by flow cytometry, cells were grown in AB minimal medium supplemented with 0.2% glycerol or in LB medium as indicated. Prior to flow cytometry, cells were treated with 300 μg/ml rifampicin (to stop further replication initiations) and 3.6 μg/ml cephalexin (to stop further cell divisions). Flow cytometry was performed as described previously (Lobner-Olesen *et al*., 1989), using a Bryte HS instrument (Bio-Rad). Chromosomal replication time was measured by flow cytometry essentially as described previously (Bernander and Nordstrom, 1990).

Supplementary data

Supplementary data are available at *The EMBO Journal* Online.

Acknowledgements

We thank P.de Boer for the donation of PB103 and PB114. This work was supported by the Danish Biotechnology Instrument Centre (DABIC), The Danish Natural Research Council and The Novo Nordic Foundation.

References

Aussel,L., Barre,F.X., Aroyo,M., Stasiak,A., Stasiak,A.Z. and Sherratt,D. (2002) FtsK is a DNA motor protein that activates chromosome dimer resolution by switching the catalytic state of the XerC and XerD recombinases. *Cell*, **108**, 195–205.

Bernander,R. and Nordstrom,K. (1990) Chromosome replication does not trigger cell division in *E. coli*. *Cell*, **60**, 365–374.

Bork,P., Sander,C. and Valencia,A. (1992) An ATPase domain common to prokaryotic cell cycle proteins, sugar kinases, actin, and hsp70 heat shock proteins. *Proc. Natl Acad. Sci. USA*, **89**, 7290–7294.

Carballido-Lopez,R. and Errington,J. (2003) The bacterial cytoskeleton: *in vivo* dynamics of the actin-like protein Mbl of *Bacillus subtilis*. *Dev. Cell*, **4**, 19–28.

Casadaban,M.J. and Cohen,S.N. (1980) Analysis of gene control signals by DNA fusion and cloning in *Escherichia coli*. *J. Mol. Biol.*, **138**, 179–207.

Daniel,R.A. and Errington,J. (2003) Control of cell morphogenesis in bacteria: two distinct ways to make a rod-shaped cell. *Cell*, **113**, 767–776.

Datsenko,K.A. and Wanner,B.L. (2000) One-step inactivation of chromosomal genes in *Escherichia coli* K-12 using PCR products. *Proc. Natl Acad. Sci. USA*, **97**, 6640–6645.

de Boer,P.A., Crossley,R.E. and Rothfield,L.I. (1989) A division inhibitor and a topological specificity factor coded for by the minicell locus determine proper placement of the division septum in *E. coli*. *Cell*, **56**, 641–649.

De Pedro,M.A., Donachie,W.D., Holtje,J.V. and Schwarz,H. (2001) Constitutive septal murein synthesis in *Escherichia coli* with impaired activity of the morphogenetic proteins RodA and penicillin-binding protein 2. *J. Bacteriol.*, **183**, 4115–4126.

Doi,M., Wachi,M., Ishino,F., Tomioka,S., Ito,M., Sakagami,Y., Suzuki,A. and Matsuhashi,M. (1988) Determinations of the DNA sequence of the *mreB* gene and of the gene products of the mre region that function in formation of the rod shape of *Escherichia coli* cells. *J. Bacteriol.*, **170**, 4619–4624.

Draper,G.C. and Gober,J.W. (2002) Bacterial chromosome segregation. *Annu. Rev. Microbiol.*, **56**, 567–597.

Dworkin,J. and Losick,R. (2002) Does RNA polymerase help drive chromosome segregation in bacteria? *Proc. Natl Acad. Sci. USA*, **99**, 14089–14094.

Gerdes,K., Moller-Jensen,J. and Jensen R.B (2000) Plasmid and chromosome partitioning: surprises from phylogeny. *Mol. Microbiol.*, **37**, 455–466.

Glaser,P., Sharpe,M.E., Raether,B., Perego,M., Ohlsen,K. and Errington,J. (1997) Dynamic, mitotic-like behavior of a bacterial protein required for accurate chromosome partitioning. *Genes Dev.*, **11**, 1160–1168.

Gordon,G.S. and Wright,A. (1998) DNA segregation: putting chromosomes in their place. *Curr. Biol.*, **8**, R925–R927.

Gordon,G.S. and Wright,A. (2000) DNA segregation in bacteria. *Annu. Rev. Microbiol.*, **54**, 681–708.

Gordon,G.S., Sitnikov,D., Webb,C.D., Teleman,A., Straight,A., Losick,R., Murray,A.W. and Wright,A. (1997) Chromosome and low copy plasmid segregation in *E. coli*: visual evidence for distinct mechanisms. *Cell*, **90**, 1113–1121.

Gotfredsen,M. and Gerdes,K. (1998) The *Escherichia coli* relBE genes belong to a new toxin–antitoxin gene family. *Mol. Microbiol.*, **29**, 1065–1076.

Guzman,L.M., Belin,D., Carson,M.J. and Beckwith,J. (1995) Tight regulation, modulation, and high-level expression by vectors

containing the arabinose PBAD promoter. *J. Bacteriol.*, **177**, 4121–4130.
Harry,E.J., Pogliano,K. and Losick,R. (1995) Use of immunofluorescence to visualize cell-specific gene expression during sporulation in *Bacillus subtilis*. *J. Bacteriol.*, **177**, 3386–3393.
Hayes,F. (2000) The partition system of multidrug resistance plasmid TP228 includes a novel protein that epitomizes an evolutionarily distinct subgroup of the ParA superfamily. *Mol. Microbiol.*, **37**, 528–541.
Jacob,F., Brenner,S. and Cuzin,F. (1963) On the regulation of DNA replication in bacteria. *Cold Spring Harbor Symp. Quant. Biol.*, **23**, 329–348.
Jensen,R.B. and Gerdes,K. (1997) Partitioning of plasmid R1. The ParM protein exhibits ATPase activity and interacts with the centromere-like ParR–parC complex. *J. Mol. Biol.*, **269**, 505–513.
Jensen,R.B. and Gerdes,K. (1999) Mechanism of DNA segregation in prokaryotes: ParM partitioning protein of plasmid R1 co-localizes with its replicon during the cell cycle. *EMBO J.*, **18**, 4076–4084.
Jensen,R.B. and Shapiro,L. (1999) Chromosome segregation during the prokaryotic cell division cycle. *Curr. Opin. Cell Biol.*, **11**, 726–731.
Jones,L.J., Carballido-Lopez,R. and Errington,J. (2001) Control of cell shape in bacteria: helical, actin-like filaments in *Bacillus subtilis*. *Cell*, **104**, 913–922.
Lemon,K.P. and Grossman,A.D. (2000) Movement of replicating DNA through a stationary replisome. *Mol. Cell*, **6**, 1321–1330.
Lemon,K.P. and Grossman,A.D. (2001) The extrusion-capture model for chromosome partitioning in bacteria. *Genes Dev.*, **15**, 2031–2041.
Lewis,P.J. and Errington,J. (1997) Direct evidence for active segregation of *oriC* regions of the *Bacillus subtilis* chromosome and co-localization with the SpoOJ partitioning protein. *Mol. Microbiol.*, **25**, 945–954.
Li,Y., Sergueev,K. and Austin,S. (2002) The segregation of the *Escherichia coli* origin and terminus of replication. *Mol. Microbiol.*, **46**, 985–996.
Lin,D.C. and Grossman,A.D. (1998) Identification and characterization of a bacterial chromosome partitioning site. *Cell*, **92**, 675–685.
Lobner-Olesen,A., Skarstad,K., Hansen,F.G., von Meyenburg,K. and Boye,E. (1989) The DnaA protein determines the initiation mass of *Escherichia coli* K-12. *Cell*, **57**, 881–889.
Moller-Jensen,J., Jensen,R.B., Lowe,J. and Gerdes,K. (2002) Prokaryotic DNA segregation by an actin-like filament. *EMBO J.*, **21**, 3119–3127.
Niki,H. and Hiraga,S. (1998) Polar localization of the replication origin and terminus in *Escherichia coli* nucleoids during chromosome partitioning. *Genes Dev.*, **12**, 1036–1045.
Niki,H., Jaffe,A., Imamura,R., Ogura,T. and Hiraga,S. (1991) The new gene *mukB* codes for a 177 kd protein with coiled-coil domains involved in chromosome partitioning of *E. coli*. *EMBO J.*, **10**, 183–193.
Niki,H., Yamaichi,Y. and Hiraga,S. (2000) Dynamic organization of chromosomal DNA in *Escherichia coli*. *Genes Dev.*, **14**, 212–223.
Norris,V. (1995) Hypothesis: chromosome separation in *Escherichia coli* involves autocatalytic gene expression, transertion and membrane-domain formation. *Mol. Microbiol.*, **16**, 1051–1057.
Rodionov,O., Lobocka,M. and Yarmolinsky,M. (1999) Silencing of genes flanking the P1 plasmid centromere. *Science*, **283**, 546–549.
Sawitzke,J.A. and Austin,S. (2000) Suppression of chromosome segregation defects of *Escherichia coli* muk mutants by mutations in topoisomerase I. *Proc. Natl Acad. Sci. USA*, **97**, 1671–1676.
Sharpe,M.E. and Errington,J. (1999) Upheaval in the bacterial nucleoid. An active chromosome segregation mechanism. *Trends Genet.*, **15**, 70–74.
Shih,Y.L., Le,T. and Rothfield,L. (2003) Division site selection in *Escherichia coli* involves dynamic redistribution of Min proteins within coiled structures that extend between the two cell poles. *Proc. Natl Acad. Sci. USA*, **100**, 7865–7870.
Skarstad,K., Boye,E. and Steen,H.B. (1986) Timing of initiation of chromosome replication in individual *Escherichia coli* cells. *EMBO J.*, **5**, 1711–1717.
Teleman,A.A., Graumann,P.L., Lin,D.C.H., Grossman,A.D. and Losick,R. (1998) Chromosome arrangement within a bacterium. *Curr. Biol.*, **8**, 1102–1109.
van den Ent,F., Amos,L.A. and Lowe,J. (2001) Prokaryotic origin of the actin cytoskeleton. *Nature*, **413**, 39–44.
van den Ent,F., Moller-Jensen,J., Amos,L.A., Gerdes,K. and Lowe,J. (2002) F-actin-like filaments formed by plasmid segregation protein ParM. *EMBO J.*, **21**, 6935–6943.
Van Helvoort,J.M. and Woldringh,C.L. (1994) Nucleoid partitioning in *Escherichia coli* during steady-state growth and upon recovery from chloramphenicol treatment. *Mol. Microbiol.*, **13**, 577–583.
Wachi,M. and Matsuhashi,M. (1989) Negative control of cell division by *mreB*, a gene that functions in determining the rod shape of *Escherichia coli* cells. *J. Bacteriol.*, **171**, 3123–3127.
Wachi,M., Doi,M., Tamaki,S., Park,W., Nakajima-Iijima,S. and Matsuhashi,M. (1987) Mutant isolation and molecular cloning of mre genes, which determine cell shape, sensitivity to mecillinam, and amount of penicillin-binding proteins in *Escherichia coli*. *J. Bacteriol.*, **169**, 4935–4940.
Webb,C.D., Teleman,A., Gordon,S., Straight,A., Belmont,A., Lin,D.C., Grossman,A.D., Wright,A. and Losick,R. (1997) Bipolar localization of the replication origin regions of chromosomes in vegetative and sporulating cells of B. subtilis. *Cell*, **88**, 667–674.
Webb,C.D., Graumann,P.L., Kahana,J.A., Teleman,A.A., Silver,P.A. and Losick,R. (1998) Use of time-lapse microscopy to visualize rapid movement of the replication origin region of the chromosome during the cell cycle in *Bacillus subtilis*. *Mol. Microbiol.*, **28**, 883–892.
Weitao,T., Nordstrom,K. and Dasgupta,S. (1999) Mutual suppression of mukB and seqA phenotypes might arise from their opposing influences on the *Escherichia coli* nucleoid structure. *Mol. Microbiol.*, **34**, 157–168.
Woldringh,C.L. (2002) The role of co-transcriptional translation and protein translocation (transertion) in bacterial chromosome segregation. *Mol. Microbiol.*, **45**, 17–29.
Woldringh,C.L., Zaritsky,A. and Grover,N.B. (1994) Nucleoid partitioning and the division plane in *Escherichia coli*. *J. Bacteriol.*, **176**, 6030–6038.
Wu,L.J. and Errington,J. (2002) A large dispersed chromosomal region required for chromosome segregation in sporulating cells of *Bacillus subtilis*. *EMBO J.*, **21**, 4001–4011.
Yamaichi,Y. and Niki,H. (2000) Active segregation by the *Bacillus subtilis* partitioning system in *Escherichia coli*. *Proc. Natl Acad. Sci. USA*, **97**, 14656–14661.

Received June 3, 2003; revised August 1, 2003; accepted August 12, 2003